Reversible Carbon−Carbon Double Bond Cleavage of a Ketene Ligand at a Single Iridium(I) Center: A Theoretical Study§

Heiko Urtel,† Galina A. Bikzhanova,‡ Douglas B. Grotjahn,*,‡ and Peter Hofmann*,†

Organisch-Chemisches Institut der Ruprecht-Karls-Universität Heidelberg, Im Neuenheimer Feld 270, D-69120 Heidelberg, Germany, and Department of Chemistry, San Diego State University, 5500 Campanile Drive, San Diego, California 92182-1030

Received June 11, 2001

Modeling the chemistry of ketene complex {κ^2-(*t*-Bu)$_2$PCH$_2$P(*t*-Bu)$_2$}IrCl[η^2-(*C*,*C*)-Ph$_2$C=C=O] (**1**), DFT studies have been carried out for (κ^2-H$_2$PCH$_2$PH$_2$)IrCl[η^2-(*C*,*C*)-H$_2$C=C=O] (**A**), for cation (κ^2-H$_2$PCH$_2$PH$_2$)Ir[η^2-(*C*,*C*)-CH$_2$=C=O]$^+$ (**B**), for its carbene carbonyl isomer (κ^2-H$_2$PCH$_2$PH$_2$)Ir(CH$_2$)(CO)$^+$ (**C**), and for their interconversion by intramolecular C=C double bond cleavage/formation. A qualitative MO analysis from extended Hückel calculations shows the C=C cleavage and formation to be symmetry allowed at a d^8-ML$_2$ late transition metal template. For the two iridium model complexes **B** and **C** the process is calculated by DFT to be reversible, with activation barriers of 17.3 kcal mol^{-1} toward the more stable carbonyl carbene system and 25.1 kcal mol^{-1} for the reverse reaction, respectively. This is in line with experimental observations for **1**, which generates {κ^2-(*t*-Bu)$_2$PCH$_2$P(*t*-Bu)$_2$}Ir(CPh$_2$)(CO)$^+$ (**3**) upon chloride abstraction and regenerates **1** after the addition of chloride. QM/MM calculations of the ONIOM type have been employed for the real systems **1** and **3**, to take into account and to evaluate the role of steric effects and to allow a validation of theoretical results by comparing computed and X-ray-determined structures. Contrasting the iridium case, the analogous rhodium ketene complex (κ^2-H$_2$PCH$_2$PH$_2$)Rh[η^2-(*C*,*C*)-CH$_2$=C=O]$^+$ (**G**) is computed to be favored by 8.0 kcal mol^{-1} compared to its carbene carbonyl isomer (κ^2-H$_2$PCH$_2$PH$_2$)Rh(CH$_2$)(CO)$^+$ (**H**), with a barrier of 22.9 kcal mol^{-1} for the endothermic C=C cleavage step. Conceivable dynamic processes were treated theoretically for the temperature dependence of NMR line shapes of carbene complex {κ^2-(*t*-Bu)$_2$PCH$_2$P(*t*-Bu)$_2$}Ir(CPh$_2$)(CO)$^+$ (**3**). A comparison with the experimental data suggests a plausible pathway for the observed exchange of the two P centers.

Introduction

Metal-centered carbon−carbon bond cleavage and bond formation processes are at the very heart of stoichiometric and catalytic transition metal mediated organic synthesis. While breaking of C−C single bonds by oxidative addition[1] and—in particular—the making of C−C single bonds by reductive elimination reactions[2] represent well-established transformations of organic molecules involving metal centers, the direct cleavage of alkene and alkyne C−C multiple bonds and its reverse, the formation of carbon−carbon multiple bonds from carbene, carbyne, carbonyl, or related C$_1$ fragments within the coordination sphere of a single transition metal center, are much less common. Note that olefin and alkyne bond dissociation and reassembly by metal-catalyzed metathesis do not belong to this category, because metathesis occurs through a different mechanistic pathway.[3] Some olefin splitting reactions leading to metal bis(carbene) complexes have been known since the 1970s for very electron-rich, e.g., tetraamino-substituted, alkenes.[4] Isocyanide and carbon monoxide coupling reactions have been reported, resulting in alkyne ligand formation, but these processes are not single-step transformations and they are irreversible.[5] *Cis*-carbyne−carbonyl ligand sets have been converted to metal-bound ketenyl ligands[6] and, pertinent to the present study, the related process of carbene carbonyl

§ Dedicated to Prof. Rolf Gleiter on the occasion of his 65th birthday.

† Universität Heidelberg.

‡ San Diego State University.

(1) *Activation of Unreactive Bonds and Organic Synthesis*; Murai, S., Ed.; Springer-Verlag: New York, 1999; Vol. 3, and references therein.

(2) Collman, J. P.; Hegedus, L. S.; Norton, J. R.; Finke, R. G. *Principles and Applications of Organotransition Metal Chemistry*; University Science Books: Mill Valley, CA, 1987.

(3) (a) Fürstner, A. *Angew. Chem., Int. Ed.* **2000**, *39*, 3012. (b) *Topics in Organometallic Chemistry*; Fürstner, A., Ed.; Springer: Berlin, 1998; Vol. 1. (c) Trnka, T. M.; Grubbs, R. G. *Acc. Chem. Res.* **2001**, *34*, 18.

(4) For examples see: (a) Lappert, M. F.; Pye, P. L.; McLaughlin G. *J. Chem. Soc., Dalton Trans.* **1977**, 1272. (b) Hitchcock, P. B.; Lappert, M. F.; Pye, P. L. *J. Chem. Soc., Dalton Trans.* **1977**, 2160. (c) Rieke, R. D.; Kojima, H.; Öfele, K. *J. Am. Chem. Soc.* **1976**, *98*, 6735.

(5) (a) Filippou, A. C.; Lungwitz, B.; Kociok-Köhn, G. *Eur. J. Inorg. Chem.* **1999**, 1905, and references therein. (b) Rehder, D.; Böttcher, C.; Collazo, C.; Hedelt, R.; Schmidt, H. *J. Organomet. Chem.* **1999**, *585*, 294, and references therein. (c) Carnahan, E. M.; Lippard, S. J. *J. Am. Chem. Soc.* **1990**, *112*, 3230. (d) Bianconi, P. A.; Williams, I. D.; Engeler, M. P.; Lippard, S. J. *J. Am. Chem. Soc.* **1986**, *108*, 311. (e) Giandomenico, C. M.; Lam, C. T.; Lippard, S. J. *J. Am. Chem. Soc.* **1982**, *104*, 1263.

10.1021/om010503t CCC: $20.00
Publication on Web 08/07/2001

Scheme 1

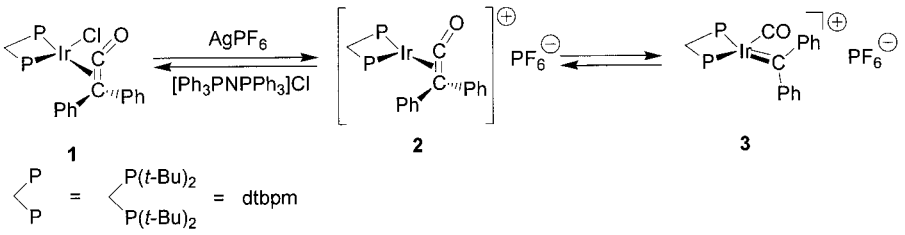

coupling has been postulated as a potential pathway to metal-bound ketenes. In fact, several examples of CO−carbene coupling reactions building up ketene ligands at a single metal center are known.[7] Their photochemically induced versions, using chromium carbene complexes, have found prominent application in β-lactam synthesis,[8] but the reverse reaction of ketene dismantling with formation of CO−carbene complexes so far has only been observed on multinuclear complexes.[9] Generally, transition metal−ketene complexes[10] are viewed as potential intermediates in several cleavage and formation processes of C−C double bonds.[11] They serve as model compounds for CO reduction in Fischer−Tropsch chemistry,[12] for CO_2 fixation and functionalization,[13] and in transformations of metal-carbene−CO complexes.[14] Some mononuclear metal carbene complexes have been reported to react to metal carbonyls and alkenes, presumably via ketene intermediates.[15]

Recently, Grotjahn reported the first system in which reversible ketene cleavage and carbene−CO coupling can be observed at a single metal (Scheme 1).[16] Dissociation of the C=C bond in the diphenylketene complex (κ^2-dtbpm)IrCl[η^2-*(C,C)*-$Ph_2C{=}C{=}O$] (**1**, dtbpm = $(t\text{-Bu})_2PCH_2P(t\text{-Bu})_2$, bis(di-*tert*-butylphosphino)-methane) can be induced by chloride abstraction with $AgPF_6$ to form the carbene−CO species (κ^2-dtbpm)Ir-$(CPh_2)(CO)^+$ (**3**), probably via the formation of the three-coordinate ketene intermediate (κ^2-dtbpm)Ir[η^2-*(C,C)*-$Ph_2C{=}C{=}O]^+$ (**2**). Addition of chloride anions to solutions of **3** regenerates the neutral ketene complex **1**. Both **1** and **3** were completely characterized spectroscopically in solution and by X-ray analysis in the solid state.

Despite various experimental examples of C−C double and triple bond cleavage and formation reactions at metal centers, only very little is known about reaction mechanisms and energetic aspects of these processes, and theoretical studies are even more scarce. In 1982, Hoffmann et al. reported a very instructive, qualitative, and transferable analysis for coupling methylenes and methynes at a metal center, based upon extended Hückel calculations and MO symmetry considerations,[17] followed later by a similar discussion for isocyanide and CO coupling to alkynes.[18] A study of aminocarbyne coupling at a tungsten fragment by Filippou et al.[19] has also appeared. Olefin substituent effects upon barriers to alkene splitting and carbene coupling reactions were treated theoretically by one of the present authors,[20] and the symmetry-allowedness of these transformations was found to depend on the substituents of the carbene/olefin pair. As to carbene carbonyl coupling and ketene splitting, Morokuma et al. have published an interesting ab initio study for the neutral ketene complex model

(6) (a) Kreissl, F. R. In *Transition Metal Carbyne Complexes*; Fischer, H., Hofmann, P., Kreissl, F. R., Schrock, R. R., Schubert, U., Weiss, K. VCH: Weinheim, Germany, 1988; p 59. (b) Sheridan, J. B.; Pourreau, D. B.; Geoffroy, G. L.; Rheingold, A. L. *Organometallics* **1988**, *7*, 289. (c) Mayr, A.; McDermott, G. A.; Dorries, A. M.; Van Engen, D. *Organometallics* **1987**, *6*, 1503. (d) Mayr, A.; McDermott, Dorries, A. M.; Holder, A. K. *J. Am. Chem. Soc.* **1986**, *108*, 310. (e) Birdwhistell, K. R.; Tonker, T. L.; Templeton, J. L. *J. Am. Chem. Soc.* **1985**, *107*, 4474.

(7) (a) Herrmann, W. A. *Angew. Chem., Int. Ed. Engl.* **1978**, *17*, 800. (b) Bodnar, T. W.; Cutler, A. R. *J. Am. Chem. Soc.* **1983**, *105*, 5926. (c) Gallop, M. A.; Roper, W. R. *Adv. Organomet. Chem.* **1988**, *25*, 121. (d) Schwab, P.; Mahr, N.; Wolf, J.; Werner, H. *Angew. Chem., Int. Ed. Engl.* **1993**, *32*, 1480. (e) Werner, H. *J. Organomet. Chem.* **1995**, *500*, 331. (f) Bleuel, E. Laubender, M.; Weberndörfer, B.; Werner, H. *Angew. Chem., Int. Ed.* **1999**, *38*, 156.

(8) (a) *Transition Metals in the Synthesis of Complex Molecules*; University Science: Mill Valley, CA, p 151. (b) *Organische Synthese mit Übergangsmetallen*; Hegedus, L. S., Ed.; VCH: Weinheim, Germany, 1995; p 157. (c) Hegedus, L. S.; deWeck, G.; D'Andrea, S. *J. Am. Chem. Soc.* **1988**, *110*, 2122.

(9) (a) Hong, P.; Nishii, N.; Sonogashira, K.; Hagihara, N. *J. Chem. Soc., Chem. Commun.* **1972**, 993. (b) Yamamoto, T.; Garber, A. R.; Wilkinson, J. R.; Boss, C. B.; Streib, W. E.; Todd, L. J. *J. Chem. Soc., Chem. Commun.* **1974**, 354. (c) Arce, A. J.; Deeming, A. J. *J. Chem. Soc., Chem. Commun.* **1982**, 364. (d) Holmgren, J. S.; Shapley, J. R.; Wilson, S. R.; Pennington, W. T. *J. Am. Chem. Soc.* **1986**, *108*, 508.

(10) (a) Geoffroy, G. L.; Bassner, S. L. *Adv. Organomet. Chem.* **1988**, *28*, 1. (b) Hofmann, P.; Perez-Moya, L. A.; Steigelmann, O.; Riede, J. *Organometallics* **1992**, *11*, 1167, and references therein. (c) Tidwell, T. T. *Acc. Chem. Res.* **1990**, *23*, 273. (d) Tidwell, T. T. *Ketenes*; Wiley: New York; 1995.

(11) (a) Fachinetti, G.; Biran, C.; Floriani, C.; Villa, A. C. Guastini, C. *Inorg. Chem.* **1978**, *17*, 2995. (b) Kim, O. K.; Wulff, W. D.; Jiang, W.; Ball, R. G. *J. Org. Chem.* **1993**, *58*, 5571. (c) Harvey, D. F.; Grenzer, E. M.; Gantzel, P. K. *J. Am. Chem. Soc.* **1994**, *42*, 6719. (d) Weston, W. S.; Lightfoot, P.; Cole-Hamilton, D. J. *J. Organomet. Chem.* **1998**, *553*, 473.

(12) (a) Henrici-Olivé, G.; Olivé, S. *J. Mol. Catal.* **1983**, *18*, 367. (b) Rofer-DePoorter, C. K. *Chem. Rev.* **1981**, *81*, 447. (c) Herrmann, W. *Angew. Chem., Int. Ed. Engl.* **1981**, *21*, 117. (d) Wolczanski, P. T.; Bercaw, J. E. *Acc. Chem. Res.* **1980**, *13*, 121. (e) Muetterties, E. L.; Stein, J. *Chem. Rev.* **1979**, *79*, 479. (f) Masters, C. *Adv. Organomet. Chem.* **1979**, *17*, 61. (g) Blyholder, G.; Emmett, P. H. *J. Phys. Chem.* **1960**, *64*, 470.

(13) (a) Darensbourg, D. J.; Kudaroski, R. A. *Adv. Organomet. Chem.* **1983**, *22*, 129. (b) Ibers, J. A. *Chem. Soc. Rev.* **1982**, *11*, 57. (c) Dötz, K. H. *Nachr. Chem., Technol. Lab.* **1990**, *38*, 1388.

(14) (a) de Meijere, A.; Schirmer, H.; Duetsch, M. *Angew. Chem., Int. Ed.* **2000**, *39*, 3964. (b) Schmalz, H.-G. *Nachr. Chem., Technol. Lab.* **1994**, *42*, 608. (c) Hegedus, L. S. In *Comprehensive Organometallic Chemistry II*; Abel, E. W., Stone, F. G. A., Wilkinson, G., Eds.; Pergamon: Oxford, 1995; Chapter 5.4, p 549. (d) Wulff, W. D. In *Comprehensive Organometallic Chemistry II*; Abel, E. W., Stone, F. G. A., Wilkinson, G., Pergamon: Oxford, 1995; Chapter 5.3, p 469. (e) Harvey, D. F.; Grenzer, E. M.; Gantzel, P. K. *J. Am. Chem. Soc.* **1994**, *116*, 6719. (f) Merlic, C. A.; Xu, D.; Gladstone, B. G. *J. Org. Chem.* **1993**, *58*, 583.

(15) (a) Fischer, H. *Angew. Chem.* **1983**, *95*, 913. (b) Miyashita, A.; Shitara, H.; Nohira, H. *Organometallics* **1985**, *4*, 1463. (c) Miyashita, A.; Nohira, H.; Sugai, R. *Chem. Lett.* **1988**, 1403. (d) Miyashita, A.; Sugai, R.; Yamamoto, J. *J. Organomet. Chem.* **1992**, *428*, 239.

(16) (a) Grotjahn, D. B.; Bikzhanova, G. A.; Collins, L. S. B.; Concolino, T.; Lam, K.-C.; Rheingold, A. L. *J. Am. Chem. Soc.* **2000**, *122*, 5222. (b) This fascinating transformation has been highlighted recently: Werner, H.; Bleuel, E. *Angew. Chem., Int. Ed.* **2001**, *40*, 145.

(17) (a) Hoffmann, R.; Wilker, C. N.; Eisenstein, O. *J. Am. Chem. Soc.* **1982**, *104*, 632. (b) Eisenstein, O.; Hoffmann, R.; Wilker, C. N. *Nouv. J. Chim.* **1983**, *7*, 535.

(18) Hoffmann, R.; Wilker, C. N.; Lippard, S. J.; Templeton, J. L.; Brower, D. C. *J. Am. Chem. Soc.* **1983**, *105*, 146.

(19) Filippou, A. C.; Hofmann, P.; Kiprof, P.; Schmidt, H. R.; Wagner, C. *J. Organomet. Chem.* **1993**, *459*, 233.

(20) Hofmann, P. *Quantum Chemistry: The Challenge of Transition Metals and Coordination Chemistry*; Veillard, A., Ed.; NATO ASI Series; D. Reidel Publishing Co.: Amsterdam, 1986; Vol. 176, p 253.

Scheme 2

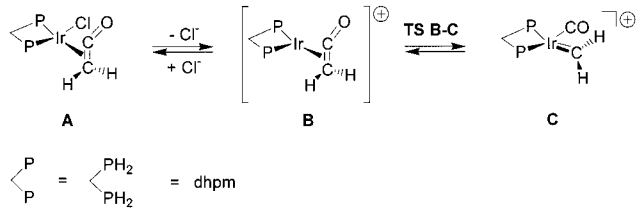

system $(H_3P)_2Pt[\eta^2\text{-}(C,C)\text{-}H_2C{=}C{=}O]$, leading to the carbene−CO complex *cis*-$(H_3P)_2Pt(CH_2)(CO)$ (MP2//RHF, double-ξ basis for Pt, 3-21G for C, H, O, and STO-2G for PH_3).[21] Their work was motivated by experimental work of Miyashita et al., from which facile $CO-CH_2$ coupling to ketene at bisphosphine-ligated Ni(0), Pd(0), and Pt(0) centers was inferred.[22] The computational results for the Pt(0) system with its d^{10}-ML_2 metal fragment $(H_3P)_2Pt$, however, left some open questions with respect to the feasibility and energetic accessibility of such a process. The energy barrier of 37 kcal mol^{-1} calculated by Morokuma et al. for endothermic C=C cleavage was found to be much larger than the barrier computed for dissociating the ketene ligand of the metal (19 kcal mol^{-1}; binding energy 13 kcal mol^{-1}). The carbene carbonyl complex lies 28 kcal mol^{-1} higher in energy than the ketene system; the barrier toward the ketene formation is thus only 9 kcal mol^{-1}. These results make a ketene splitting reaction at Pt(0) (and presumably even more so at Ni(0) and Pd(0)) rather unlikely, in contradiction to the conclusions derived from experiment, while a bisphosphine carbene carbonyl Pt(0) complex should collapse irreversibly to a ketene complex. Given the level of theory at which all previous studies including Morokuma's ab initio treatment were performed, it is clear that only qualitative conclusions can be derived from these works.

It seemed therefore an interesting and challenging task to apply modern DFT methodology to take a closer look at the recent, experimentally unambiguous case of ketene cleavage and reassembly in **1** and **3**. The iridium system of Grotjahn provides an ideal starting point for theoretical investigations because here, due to the specific phosphine ligand $(t\text{-Bu})_2PCH_2P(t\text{-Bu})_2$ (dtbpm), the coupling/cleavage interconversion definitely occurs as a single-site process at the same metal fragment, and all products have been fully characterized by experiment.

In this paper we first describe a qualitative, extended Hückel and molecular orbital based analysis of C=C splitting and formation at a late transition metal ML_2 fragment,[23] which reveals that the d^8 electron count of the metal template provides the necessary prerequisite for a closed shell, symmetry-allowed process. Then we report the results of DFT calculations for the model system shown in Scheme 2, which employ dhpm (dhpm = $H_2PCH_2PH_2$, diphosphinomethane) instead of dtbpm and ketene instead of diphenylketene.

Chloride abstraction from the ketene complex model $(\kappa^2\text{-dhpm})IrCl[\eta^2\text{-}(C,C)\text{-}H_2C{=}C{=}O]$ (**A**) should yield a three-coordinate species $(\kappa^2\text{-dhpm})Ir[\eta^2\text{-}(C,C)\text{-}H_2C{=}C{=}O]^+$ (**B**) as an intermediate. From there a carbene−CO complex $(\kappa^2\text{-dhpm})Ir(CH_2)(CO)^+$ (**C**) should be accessible via a transition state **TS B-C**. The reverse coupling reaction (**C** to **A**) could then occur by trapping the intermediate **B** by addition of chloride anions. QM/MM calculations of the ONIOM type have been performed for real systems **1** and **3** in order to allow a correlation between the model systems and experimental structures. Finally the kinetic and thermochemical differences between the Ir and the analogous Rh system are addressed, the unique features of the iridium case are outlined, and the experimental observation of an interesting dynamic process in solution NMR spectra of **3** is addressed computationally by DFT.

Computational Details

Calculations were performed with the Gaussian 98 package.[24] All geometries were fully optimized using density functional theory (DFT)[25] with Becke's three-parameter hybrid exchange potential (B3)[26] and the Perdue−Wang (PW91)[27] correlation functional without symmetry or internal coordinate constraints (B3LYP[28] and BP86[29] were also applied, to evaluate the method dependence of geometries and energies, with no significant differences of results). Local minima were identified by the absence of negative eigenvalues (NIMAG = 0) in the vibrational frequency analysis. The Hessian matrix of transition state structures had only one negative eigenvalue (NIMAG = 1). For Ir, Rh, and P the Stuttgart−Dresden basis sets with the corresponding effective core potentials (replacing 60 core electrons for Ir, 28 for Rh, and 10 for P)[30,31] were applied. For phosphorus, one d polarization function with an exponent of 0.387 was added.[32] For C, O, Cl, and H the 6-31G** basis was applied.[33] All energies are zero-point corrected. The basis set

(21) Nakamura, S.; Morokuma, K. *Organometallics* **1988**, *7*, 1904.
(22) (a) Miyashita, A. Shitara, H.; Nohira, H. *J. Chem. Soc., Chem. Commun.* **1985**, 850. (b) Miyashita, A. Shitara, H.; Nohira, H. *Organometallics* **1985**, *4*, 850.
(23) A detailed, EH-based analysis for various metal fragments, d electron counts, and C=C ligand systems is to be found in: Schmidt, H. R. Ph.D. Thesis, Technische Universität München, Germany, 1988. Hofmann, P.; Schmidt, H. R. Unpublished results. See also ref 20.

(24) Frisch, M. J.; Trucks, G. W.; Schlegel, H. B.; Scuseria, G. E.; Robb, M. A.; Cheeseman, J. R.; Zakrzewski, V. G.; Montgomery, Jr., J. A.; Stratmann, R. E.; Burant, J. C.; Dapprich, S.; Millam, J. M.; Daniels, A. D.; Kudin, K. N.; Strain, M. C.; Farkas, O.; Tomasi, J.; Barone, V.; Cossi, M.; Cammi, R.; Mennucci, B.; Pomelli, C.; Adamo, C.; Clifford, S.; Ochterski, J.; Petersson, G. A.; Ayala, P. Y.; Cui, Q.; Morokuma, K.; Malick, D. K.; Rabuck, A. D.; Raghavachari, K.; Foresman, J. B.; Cioslowski, J.; Ortiz, J. V.; Stefanov, B. B.; Liu, G.; Liashenko, A.; Piskorz, P.; Komaromi, I.; Gomperts, R.; Martin, R. L.; Fox, D. J.; Keith, T.; Al-Laham, M. A.; Peng, C. Y.; Nanayakkara, A.; Gonzalez, C.; Challacombe, M.; Gill, P. M. W.; Johnson, B.; Chen, W.; Wong, M. W.; Andres, J. L.; Gonzalez, C.; Head-Gordon, M.; Replogle, E. S.; Pople, J. A. *Gaussian 98, Revision A.5*; Gaussian, Inc.: Pittsburgh, PA, 1998.
(25) (a) Hohenberg, P.; Kohn, W. P. *Phys. Rev. B* **1964**, *136*, 864. (b) Kohn, W. P.; Sham, L. J. *Phys. Rev. A* **1965**, *140*, 1133.
(26) (a) Becke, A. D. *Phys. Rev. A* **1988**, *38*, 3089. (b) Becke, A. D. *J. Chem. Phys.* **1993**, *98*, 1372. (c) Becke, A. D. *J. Chem. Phys.* **1993**, *98*, 5648.
(27) Perdue, J. P.; Wang, Y. *Phys. Rev. B* **1991**, *45*, 13244.
(28) Lee, C.; Yang; W.; Parr, R. G. *Phys. Rev. B* **1988**, *37*, 785. (b) Miehlich, B.; Savin, A.; Stoll, H.; Preuss, H. *Chem. Phys. Lett.* **1989**, *157*, 200.
(29) Perdue, J. P. *Phys. Rev.* **1986**, *33*, 8822.
(30) Andrae, D.; Häussermann, U.; Dolg, M.; Stoll, H.; Preuss, H. *Theor. Chim. Acta* **1990**, *77*, 123.
(31) Bergner, A.; Dolg, M.; Küchle, W.; Stoll, H.; Preuss, H. *Mol. Phys.* **1993**, *80*, 1431.
(32) Francl, M. M.; Pietro, W. J.; Hehre, W. J.; Binkley, J. S.; Gordon, M. S.; DeFrees, D. J.; Pople, J. A. *J. Chem. Phys.* **1982**, *77*, 3654.
(33) (a) Ditchfield, R.; Hehre, W. J.; Pople, J. A. *J. Chem. Phys.* **1971**, *54*, 724. (b) Hehre, W. J.; Ditchfield, R.; Pople, J. A. *J. Chem. Phys.* **1972**, *55*, 2257. (c) Hariharan, P. C.; Pople, J. A. *Mol. Phys.* **1974**, *27*, 209. (d) Hariharan, P. C.; Pople, J. A. *Theor. Chim. Acta* **1973**, *28*, 213. (e) Frisch, M. J.; Pople, J. A.; Bikley, J. S. *J. Phys. Chem.* **1984**, *80*, 3265.

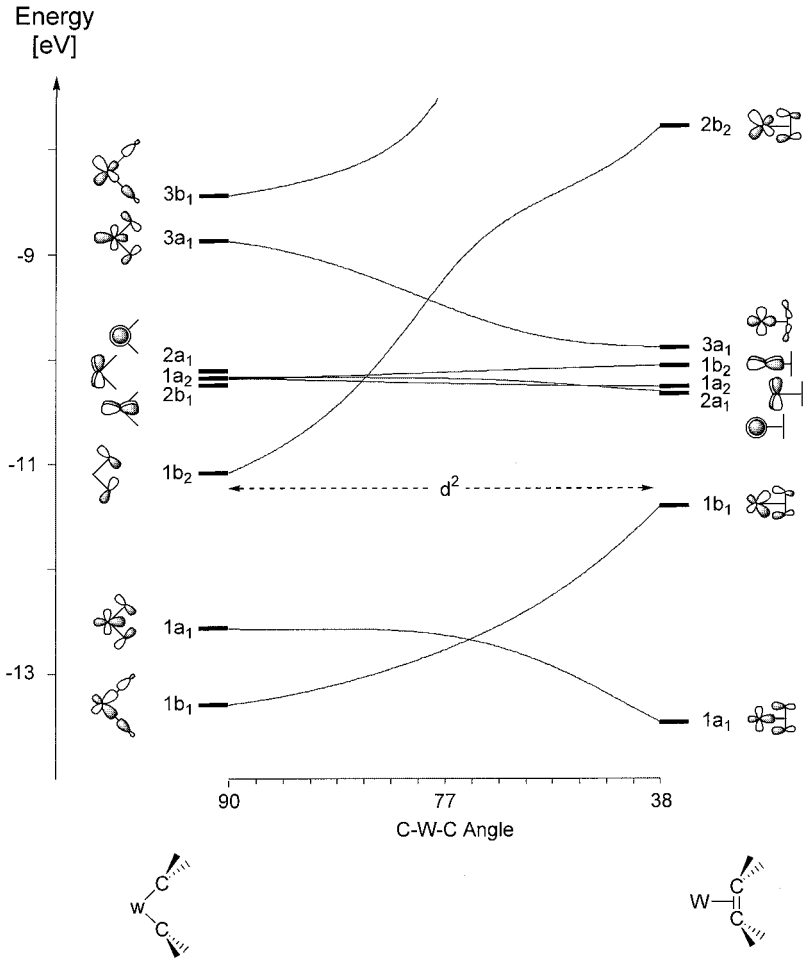

Figure 1. MO correlation diagram (EH) for an idealized C_{2v} methylene coupling/decoupling in $W(CH_2)_2$, adapted from ref 17.

superposition error (BSSE) in some cases was assessed by the counterpoise (CP) correction.[34]

QM/MM calculations of the ONIOM type[35] were performed for the real systems **1**, **2**, and **3** with the actual dtbpm ligand and $Ph_2C{=}C{=}O$. In that case, the DFT method B3PW91 was applied for the metal core (κ^2-dhpm)Ir[η^2-(*C*,*C*)-$H_2C{=}C{=}O$], using the same parameters as for the pure DFT calculation (vide supra). The *t*-Bu groups of the dtbpm ligand and the two phenyl rings of diphenylketene were calculated within the MM part using the universal force field (UFF).[36]

For details of the extended Hückel calculations[37] for Figures 1 and 2 (MO correlation diagrams) see the Supporting Information.

Results and Discussion

Qualitative MO Analysis. Although the C=C cleavage process of a metal-bound ketene ligand to form a *cis*-coordinated carbene and carbon monoxide ligand pair and the reverse carbon−carbon coupling reaction can at best retain C_s symmetry along the reaction coordinate, the basic electronic features of such an interconversion are readily apparent from the analogous transformation involving two methylene units converting to ethylene with restriction of symmetry to C_{2v}. This coupling/decoupling reaction for an unligated transition metal center, especially for tungsten in the system W(η^2-C_2H_4)/$W(CH_2)_2$, has been analyzed in depth by Hoffmann et al.[17] For the sake of a transparent and simple discussion of the present iridium case, Figure 1 displays the EH frontier orbital correlation diagram as given by those authors.

Replacing one of the two single-faced π-acceptor ligands CH_2 by the double-faced π-acceptor CO would introduce two additional orbitals, a π_{CO} and π^*_{CO} MO, orthogonal to the molecular plane, on both sides of the diagram. This does not affect the qualitative conclusions for the in-plane orbital system shown in Figure 1,[23] which is relevant for the C=C coupling/decoupling process to be discussed here. If, as in Figure 1 for the case of tungsten, the block of metal-centered d orbitals (levels $2b_1$, $1a_2$, $2a_1$) is energetically located above the out-of-phase combination $1b_2$ of the two methylene in-plane p orbitals, a least motion, C_{2v} type coupling of the two carbene ligands is symmetry-forbidden for a d electron count higher than d^2. As deduced in detail by Hoffmann et al.,[17] this remains true if two equatorial and/or two axial ligands are attached to the metal center, restoring a square-planar or octahedral coordination environment. If a less symmetric coupling itinerary or spectator ligand set only conserves C_s or implies

(34) van Duijneveldt, F. B.; van Duijneveldt-van de Rijdt, J., G., C.; M.; van Lenthe, J. H. *Chem. Rev.* **1994**, *94*, 1873.
(35) Morokuma, K. *J. Phys. Chem.* **1996**, *100*, 19357.
(36) Rappé, A. K.; Casewit, C. J.; Colwell, K. S.; Goddard, W. A., III; Skiff, W. M. *J. Am. Chem. Soc.* **1992**, *114*, 10024.
(37) (a) Hoffmann, R. *J. Chem. Phys.* **1963**, *39*, 1397. (b) Hoffmann, R.; Libscomp, W. N. *J. Chem. Phys.* **1962**, *36*, 2179. (c) Hoffmann, R.; Libscomp, W. N. *J. Chem. Phys.* **1962**, *37*, 2872.

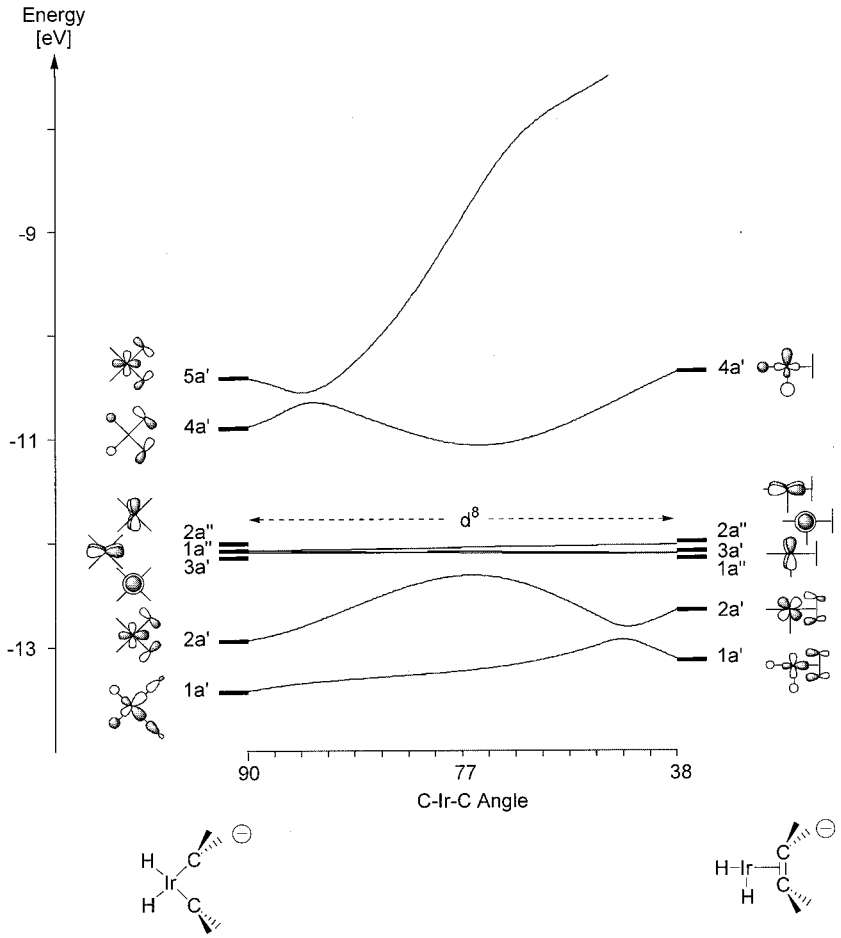

Figure 2. MO correlation diagram (EH) for coupling/decoupling of two methylene fragments at a d^8-H_2Ir^- metal template, leading from a square-planar *cis*-bis-carbene system to a T-shaped *cis*-ethylene complex under C_s symmetry.

no symmetry along the reaction coordinate, the $1b_2/3a_1$ level crossing is of course turned into an avoided crossing, which should still leave an appreciable activation barrier for an electron count exceeding d^2.

When we calculate the same type of orbital correlation diagram using the more electronegative iridium as late transition metal center, the most prominent change in comparison to Figure 1 is that the metal d block (levels $2b_1$, $1a_2$, $2a_1$) now appears *below* the crucial $1b_2$ orbital on the bis-methylene side at left. Six more d electrons can be accommodated, leading to symmetry-allowedness for a d^8 configuration. Parenthetically, we note that it should also be possible to reach the reversed energy ordering of metal d levels $2b_1$, $1a_2$, $2a_1$ and the ligand-based MO $1b_2$ by pushing up the energy of the latter. This can be achieved by strong π-donor substituents (e.g., OR, NR_2) at the carbene/olefin ligands and leads to symmetry-allowed olefin splitting reactions, as analyzed for a $Cr(CO)_4$ metal template elsewhere.[20]

Rather than a single metal center, a more realistic model system of the ketene C=C splitting and carbene/CO coupling process in Grotjahn's ketene complex (κ^2-$H_2PCH_2PH_2$)Ir[η^2-(*C*,*C*)-CH_2=C=O]$^+$ (**B**) and its carbene carbonyl isomer (κ^2-$H_2PCH_2PH_2$)Ir$(CH_2)(CO)^+$ (**C**) should contain a d^8-IrL_2 template. An extended Hückel MO correlation diagram for the simplest square-planar C_{2v} model *cis*-$H_2Ir(CH_2)_2^-$ is shown in Figure 2. Two CH_2 units again replace the carbene/CO ligand couple and two hydride ligands have been used in order to model two σ-donor ligands (e.g., phosphines). Furthermore, the d^8-ML_3 type closed-shell ethylene coupling product on the right side of Figure 2 necessarily must have a T-shaped ground state geometry. As we want to model a *cis*-chelating diphosphinomethane by the two hydride ligands, a T-structure with two *cis* hydrides has been chosen for the coupling product in Figure 2, which allows at most C_s symmetry along the simplest least-motion coupling/decoupling pathway. On the olefin side, the T-shaped structure would relax further by olefin rotation and out-of-plane bending (vide infra), but for our simplified analysis of the coupling/decoupling the C_s T-geometry is taken as the final product structure.

As apparent from Figure 2 and in contrast to Figure 1, carbon−carbon double bond formation and olefin C=C bond splitting now becomes symmetry-allowed for a closed-shell d^8 electron configuration (3a′, 1a″, 2a″ filled) of the metal center. Note that for a T-shaped olefin complex with two *trans* donor ligands (modeling for example two monodentate phosphines) C_{2v} symmetry could be conserved for Figure 2, replacing the avoided crossing of empty levels 4a′ and 5a′ in a d^8 situation by an actual crossing, as in Figure 1 for a d electron count above two.

For a d^{10} situation, where the olefin complex will have a trigonal planar (C_{2v}) structure as typically found for $L_2Pt(\eta^2$-olefin) complexes or their Ni and Pd congeners, the next level (4a′) above the d block in Figure 2 is occupied. Due to the level crossing of MOs 4a′ and 5a′, the in-plane ligand interconversion process now is symmetry-forbidden at that electron count.

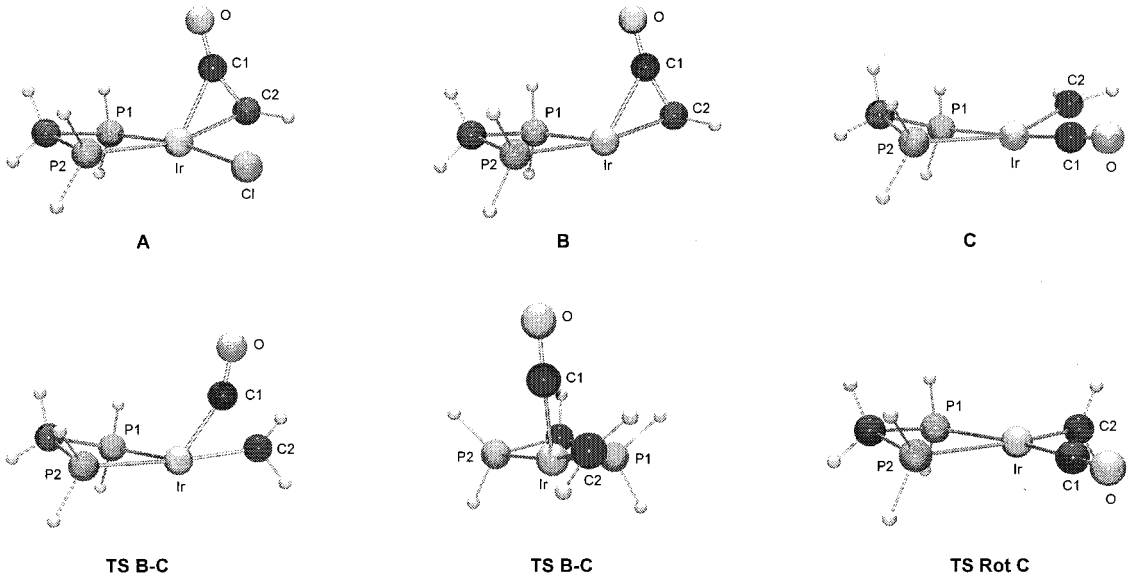

Figure 3. Calculated structures (B3PW91) of **A**, **B**, **C**, **TS B-C** (side and front view), and **TS Rot C**.

For a carbene−CO and ketene ligand system the essential features of this analysis of ligand coupling/decoupling as a function of the d electron count and electronegativity (d ionization potential, H_{ii} in EH theory) of the metal still holds. As a consequence of the unsymmetric ligand set, only avoided crossings will occur.

Our simple one-electron MO analysis thus predicts—albeit only in a qualitative sense—that a bis-ligated Ir(I) center d^8-IrL_2 should provide a suitable template for a symmetry-allowed ketene C═C splitting/coupling process and that the analogous transformations should suffer from a frontier orbital-imposed higher barrier in the case of a d^{10}-ML_2 template, e.g., in $L_2Pt[\eta^2$-*(C,C)*-ketene] complexes, in line with Morokuma's ab initio results for ketene splitting in the $(H_3P)_2Pt[\eta^2$-*(C,C)*-H_2C═C═O] model system.[21]

EH-MO correlation diagrams of course do not allow any conclusions with respect to actual activation barriers or reaction energies. Furthermore, the energetic consequences of symmetry-based restrictions derived from Woodward−Hoffmann-like MO correlation diagrams of organometallic complexes with their closer lying frontier levels are often less pronounced than for organic molecules with large HOMO−LUMO gaps. Therefore a quantitatively more reliable computational study using DFT and QM/MM (ONIOM) methods was performed for the Grotjahn complexes and for appropriate models.

DFT Calculations. Geometries of the model systems **A**, **B**, and **C** and the transition state **TS B-C** were optimized using different levels of DFT methodology (BP86, B3LYP, B3PW91) (Scheme 2, Figure 3). The ONIOM method was used for the real systems **1** and **3** and the three-coordinate intermediate **2** (Scheme 1, Figure 5). For all methods the computed minimum energy geometries are in good general agreement with the observed X-ray structures of **1** and **3**, respectively. In the following discussion we will only refer to the B3PW91 and ONIOM results for the sake of brevity.[38] Relevant geometric features of the X-ray data of **1** and **3** are compared to the ONIOM and DFT results of important species and transition states in Table 1.

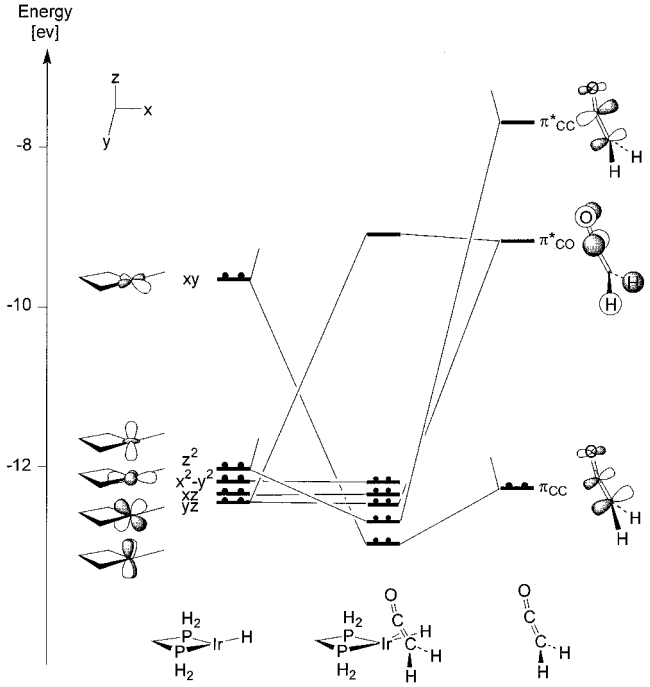

Figure 4. Qualitative frontier orbital interaction diagram (EH) for the out-of-plane η^2-*(C,C)* coordination mode of a bent ketene at a (κ^2-dhpm)IrH fragment.

The calculated structure of **A** (Figure 3) as well as the ONIOM results (Figure 5, vide infra) for the untruncated system fully reproduce the significant and unexpected deviation from a square-planar geometry, which is observed experimentally for **1**. The chlorine atom is bent out of the P_2Ir plane. As this effect is larger in the ONIOM and the X-ray structure compared to the simplified DFT model system, this seems to reflect steric effects. More importantly, the ketene C═C bond is orthogonal to and its midpoint is moved far out of this plane, in such a way as to place even the ketene CR_2 carbon (R = H, Ph) above that plane. This type of distortion, away from a square-planar structure with the center of an upright bound olefinic ligand in the metal-coligand plane, as in Zeise's salt, is a general feature, also found computationally for isoelectronic,

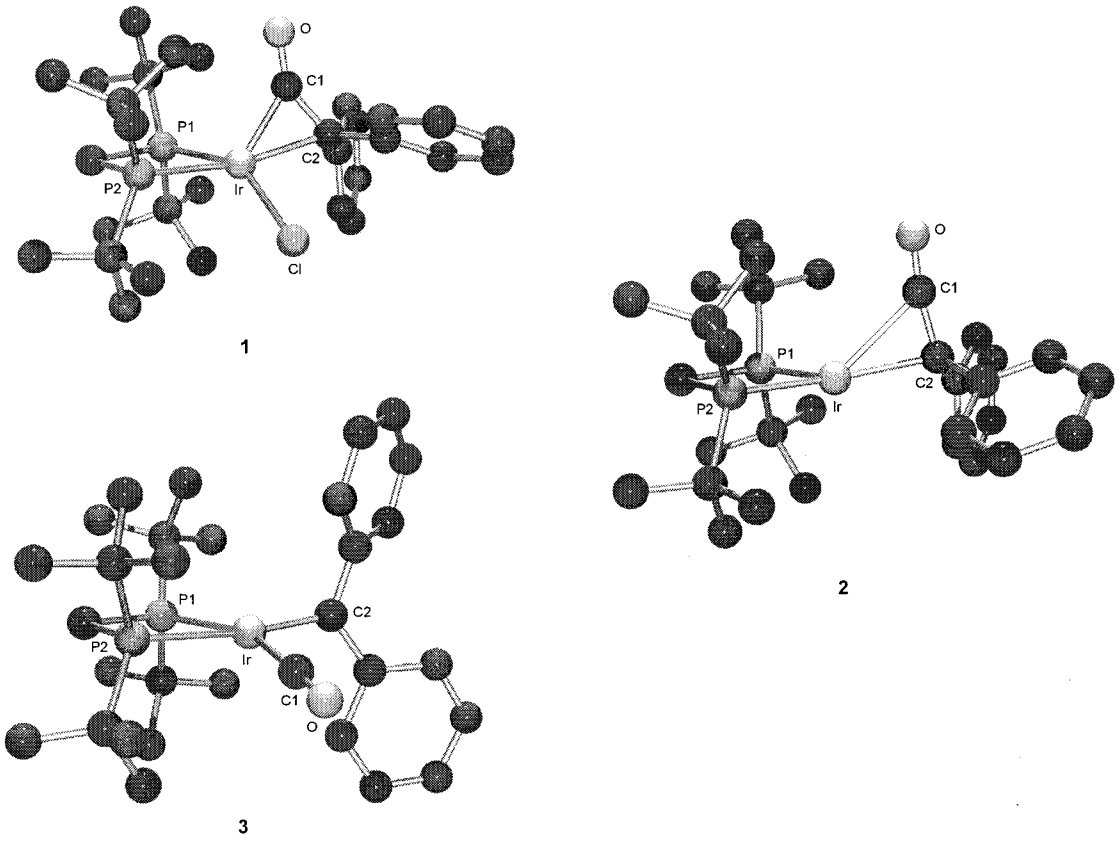

Figure 5. Calculated structures (ONIOM) for **1**, **2**, and **3**. Hydrogens omitted for clarity.

Table 1. Relevant Bond Lengths [Å] and Angles [deg] of the Calculated Structures of A, B, TS B-C, and C Compared to X-ray Structural Data for 1 and 3 and to ONIOM Data for 1, 2, and 3

parameter	**1** X-ray	**A** B3PW91	**1** ONIOM	**B** B3PW91	2 ONIOM	**TS B-C** B3PW91	**3** X-ray	**C** B3PW91	**3** ONIOM
Ir−P1	2.318(1)	2.267	2.344	2.203	2.234	2.272	2.417(2)	2.402	2.475
Ir−P2	2.383(1)	2.360	2.413	2.363	2.306	2.404	2.391(2)	2.476	2.499
Ir−C1	1.986(5)	2.028	2.025	2.128	2.469	1.897	1.859(9)	1.899	1.893
Ir−C2	2.245(4)	2.113	2.188	2.107	2.174	1.961	1.996(8)	1.893	1.905
C1−C2	1.488(7)	1.430	1.437	1.413	1.385	1.815		2.698	2.701
C1−O	1.222(6)	1.188	1.194	1.173	1.136	1.160	1.133	1.144	1.146
Ir−Cl	2.394(1)	2.352	2.356						
O−C1−C2	141.3(5)	151.7	146.7	158.6	170.4	94.4		136.2	136.7
C1−Ir−C2	40.6(2)	40.4	39.6	38.8	34.0	56.1	91.8	90.7	90.6
Ir−C1−O	139.6(4)	135.2	137.0	131.4	128.0	157.2	176.4(9)	178.9	176.8
P1−Ir−P2	73.6(1)	72.6	71.1	73.3	71.8	71.3	72.9	70.0	69.5

electron-rich olefin complexes (κ^2-dhpm)M(R)(η^2-olefin) (M = Rh, Ir; R = H, CH_3), in which ethylene or other olefins replace the ketene ligand, and chloride is substituted by a hydride or an alkyl group. This feature, actually predicted from theory, has meanwhile been established by X-ray structure determinations to be reported separately.[39] It can be rationalized by simple overlap and fragment MO arguments and is in fact readily deduced from calculations at the extended-Hückel level.

As displayed in Figure 4, an MO with predominantly metal d_{z^2} character is the HOMO of T-shaped, three-coordinate d^8-fragments of the type $P_2M(R)$ [M = Rh-(I), Ir(I)]. It is higher in energy than d_{xz} and d_{yz}, especially for strong σ donor ligands such as R = H, alkyl and for electron-rich phosphines, which interact with d_{z^2} in an antibonding manner and push it up in energy.[40] As a consequence, metal−olefin back-bonding to the π^* MO of olefins preferentially occurs and is most pronounced through d_{z^2} rather than d_{xz} or d_{yz} metal orbitals, but this becomes possible only by moving the midpoint of the double bond upward, out of the IrP_2

(38) Structural details of the important species for the BP96 and B3LYP methods are given in the Supporting Information.

(39) The synthesis and X-ray stuctures of olefin complexes (κ^2-dtbpm)Rh(R)(η^2-olefin) (R = alkyl, Cl) along with theoretical studies of these systems will be reported separately: Urtel, H.; Meier, C.; Rominger, F.; Hofmann, P. In preparation. Note that (κ^2-dmpe)Ru-$(CO)_2$ and (κ^2-dtbpe)Ru$(CO)_2$, isolelectronic chelating systems with two strong π-acceptors, also have been found not to adopt a square-planar ground state structure in matrix isolation studies and in quantum chemical calculations, respectively: (a) Whittlesey, M. K.; Perutz, R. N.; Virrels, I. G.; George, M. W. *Organometallics* **1997**, *16*, 268. (b) Gottschalk-Gaudig, T.; Huffman, J. C.; Gerard, H.; Eisenstein, O.; Caulton, K. G. *Inorg. Chem.* **2000**, *39*, 3957. (c) Gottschalk-Gaudig, T.; Huffman, J. C.; Caulton, K. G. *J. Am. Chem. Soc.* **1999**, *121*, 3242. The related nonchelate complexes $(P(t\text{-}Bu)_2Me)_2Ru(CO)_2$ and $(P(t\text{-}Bu)_2Me)_2Ru(CO)(NO)^+$ also resemble trigonal bipyramids with an empty equatorial site: (d) Ogasawara, M.; Macgregor, S. A.; Streib, W. E.; Folting, K.; Eisenstein, O.; Caulton, K. G. *J. Am. Chem. Soc.* **1996**, *118*, 10189. (e) Ogasawara, M.; Huang, D.; Streib, W. E.; Huffman, J. C.; Gallego-Planas, N.; Maseras, F.; Eisenstein, O.; Caulton, K. G. *J. Am. Chem. Soc.* **1997**, *119*, 8642.

(40) *Orbital Interactions in Chemistry*; Albright, T. A., Burdett, J. K., Whangbo, M.-H., Eds.; Wiley: New York, 1985; p 277.

plane.[41] Moreover, for the bent η^2-(*C,C*)-ketene ligand, the π^*_{CC} orbital is not weighted equally at the two carbon atoms but has a larger coefficient at the carbonyl carbon atom. This is in line with π^*_{CO}, which is orthogonal to π^*_{CC} and which is also weighted more at the carbonyl carbon atom, interacting weakly with d_{xz} and d_{yz}. This reinforces the distorted bonding mode. In a sense a distortion as found for **1** and related olefin complexes reflects the importance of their resonance description as metallacyclopropanones and metallacyclopropanes with a +III metal oxidation state and, counting the carbon atoms of the olefin or ketene as a basal and apical ligand, respectively, a square-pyramidal coordination geometry.[39] This is underlined by the fact that the ketene C−C bond in **1** is the longest known among all crystallographically characterized complexes featuring *C,C*-bound ketenes.[42]

The computed in-plane orientation of the carbene CH_2 group in the model system **C** (Figure 3), as opposed to the orthogonal orientation of the CPh_2 ligand in the real system **3**, is clearly a consequence of steric repulsion in the latter. This is confirmed by the results of the ONIOM calculations for **3**, which reproduce correctly the X-ray orientation of the carbene moiety (Figure 5). It is also in line with the computed small Ir−C2 rotational barrier of the unsubstituted CH_2 unit in **C**, which is calculated to be only 3.5 kcal mol^{-1} and to have a transition state with an orientation of the CH_2 moiety orthogonal to the P_2Ir plane (**TS Rot C**, Figure 3). The computed minimum structure of **C** has the carbene carbon atom very slightly moved out of the P_2Ir−CO plane, in contrast to the experimentally observed square-planar coordination of **3**. However, an optimization of **C**, in which the carbene CH_2 unit is kept coplanar within the square-planar ligand sphere around Ir by freezing the dihedral angle P1−Ir−P2−C2 to 0 °C, shows that this distortion costs only 0.4 kcal mol^{-1}.

Moreover, as in many dhpm model systems we have studied so far, the four-membered PCPIr chelate ring of **C** is slightly puckered. A restricted optimization of **C** with the carbon atom of the methylene bridge of the (dhpm)Ir unit forced into the plane, however, yields an energy only 0.5 kcal mol^{-1} above the fully optimized, puckered structure. Both numbers testify to a very shallow out-of plane bending potential energy surface. The QM/MM results for the dtbpm systems correctly reproduce the planar geometries of the (dtbpm)Ir chelate subunits imposed by the bulky substituents (Figure 5).

The three-coordinate iridium ketene cation **B** (Scheme 2, Figure 3), modeling the intermediate formed initially by chloride loss from **A**, shows the expected d^8-ML_3 T-shaped geometry with an η^2-(*C,C*)-coordinated ketene moiety (here, the center of the C═C bond is moved out of the P_2Ir plane as well, for the same reasons as dicussed above). The binding energy of the ketene ligand in **B** amounts to 41.1 kcal mol^{-1} (with BSSE correction it is reduced to 36.6 kcal mol^{-1}). The alternative minimum structure **D** with an η^2-(*C,O*)-coordinated ketene (Figure 8) is calculated to be 18.7 kcal mol^{-1} higher in energy than **B**. Given the intention of the present study, we have not tried to compute a transition state between **B** and **D** and the energy barriers of their interconversion, but we note in passing that η^2-(*C,O*) transition metal ketene bonding as well as mutual rearrangements between the two coordination modes have been shown to exist.[10b,43]

According to the DFT calculations, the C═C splitting reaction leading from **B** to **C** is overall exothermic by 7.8 kcal mol^{-1} (Figure 6; 6.3 kcal mol^{-1} with ONIOM for **2** to **3**). The two structures are connected by a true, quite early transition state (**TS B-C**, Figure 3), 17.3 kcal mol^{-1} higher in energy than ketene complex **B** and 25.1 kcal mol^{-1} above product **C**. In ONIOM calculations we were not able to locate a transition state due to convergence problems, which we were unable to overcome. These computed values for model systems **B** and **C** agree qualitatively with a fast and facile ketene splitting reaction of the cationic iridium ketene complex **2** after chloride abstraction from **1**. They are also in accord with a scenario in which trapping of the unsaturated ketene complex **2**, present in a small equilibrium concentration, can occur if chloride is added. Overall, our calculations strongly support the conclusion that the observed regeneration of **1** from **3** is caused by a reversible cleavage of the ketene C═C double bond and by trapping of **2** by chloride (Scheme 1).

In the iridium systems with a dtbpm spectator ligand, the strong σ-donating power of this specific diphosphinomethane certainly plays an important role for the low activation barrier and the higher relative stability of the carbene/CO isomer. The metal to ligand back-bonding to the carbene and in particular to the double-faced π-acceptor ligand CO of **3** plays a strongly stabilizing role, which is more pronounced for **3** than for the ketene system **2**, favoring **3** in the C═C coupling/decoupling equilibrium. In addition, strong metal to ketene ligand back-donation weakens the ketene C═C bond in **2**, lowering the kinetic barrier toward double bond cleavage.[44]

From a thermochemical point of view it is well known that metal carbon σ-bonds to rhodium are generally weaker than to iridium and that iridium also displays stronger metal to ligand back-bonding. It seemed interesting to compare Grotjahn's iridium system to the analogous rhodium case in which ketene complexation

(41) For olefin complexes (κ^2-dtbpm)Rh(R)(η^2-olefin) the situation becomes different, if π donor ligands replace R. For Cl instead of R, π-back-bonding to olefins occurs preferentially through d_{xz} and d_{yz}, now above d_{z^2}. Electron-rich olefins then prefer to be coordinated with the center of their CC double bond in the MP_2Cl plane. Olefins with acceptor substituents still prefer to coordinate in the "bent-up" fashion, even with a Cl π-donor co-ligand: Hofmann, P.; Urtel, H.; Meier, C.; Rominger, F. In preparation.

(42) (a) Redhouse, A. D.; Herrmann, W. A. *Angew. Chem., Int. Ed. Engl.* **1976**, *15*, 615. (b) Herrmann, W. A.; Plank, J.; Ziegler, M.; Weidenhammer, K. *J. Am. Chem. Soc.* **1979**, *101*, 3133. (c) Herrmann, W. A.; Plank, J.; Kriechbaum, G. W.; Ziegler, M. L.; Pfisterer, H.; Atwood, J. L.; Rogers, R. D. *J. Organomet. Chem.* **1984**, *264*, 327. (d) Bleuel, E.; Laubender, M.; Weberndörfer, B.; Werner, H. *Angew. Chem., Int. Ed. Engl.* **1999**, *38*, 156.

(43) For examples see: (a) Grotjahn, D. B.; Lo, H. C. *Organometallics* **1995**, *14*, 5463. (b) Miyashita, A.; Sugai, R.; Yamamoto, J. *J. Organomet. Chem.* **1992**, *428*, 238. (c) Gambarotta, S.; Pasquali, M.; Floriani, C.; Chiesi-Villa, A.; Guastini, C. *Inorg. Chem.* **1981**, *20*, 1173. (d) Galante, J. M.; Bruno, J. W.; Hazin, P. N.; Folting, K.; Huffmann, J. C. *Organometallics* **1988**, *7*, 1066. (e) Meinhart, J. O.; Santarsiero, B. D.; Grubbs, R. H. *J. Am. Chem. Soc.* **1986**, *108*, 3318. (f) Moore, E. J.; Straus, D. A.; Armentrout, J.; Santarsiero, B. D.; Grubbs, R. H. Bercaw, J. E. *J. Am. Chem. Soc.* **1983**, *108*, 2068. (g) Birk, R.; Berke, H.; Hund, H.-U.; Huttner, G.; Zsolnai, L.; Dahlenburg, L.; Behrens, U.; Sielisch, T. *J. Organomet. Chem.* **1989**, *327*, 397. (h) References 7f and 15c.

(44) Preliminary DFT results for C═C cleavage in ethylene instead of ketene at the (κ^2-dhpm)Ir^+ fragment indicate a very high barrier and a strong preference for the olefin complex side ($E_{rel} = -44.8$ kcal mol^{-1}) compared to the bis-carbene species: Urtel, H.; Hofmann, P. Unpublished results.

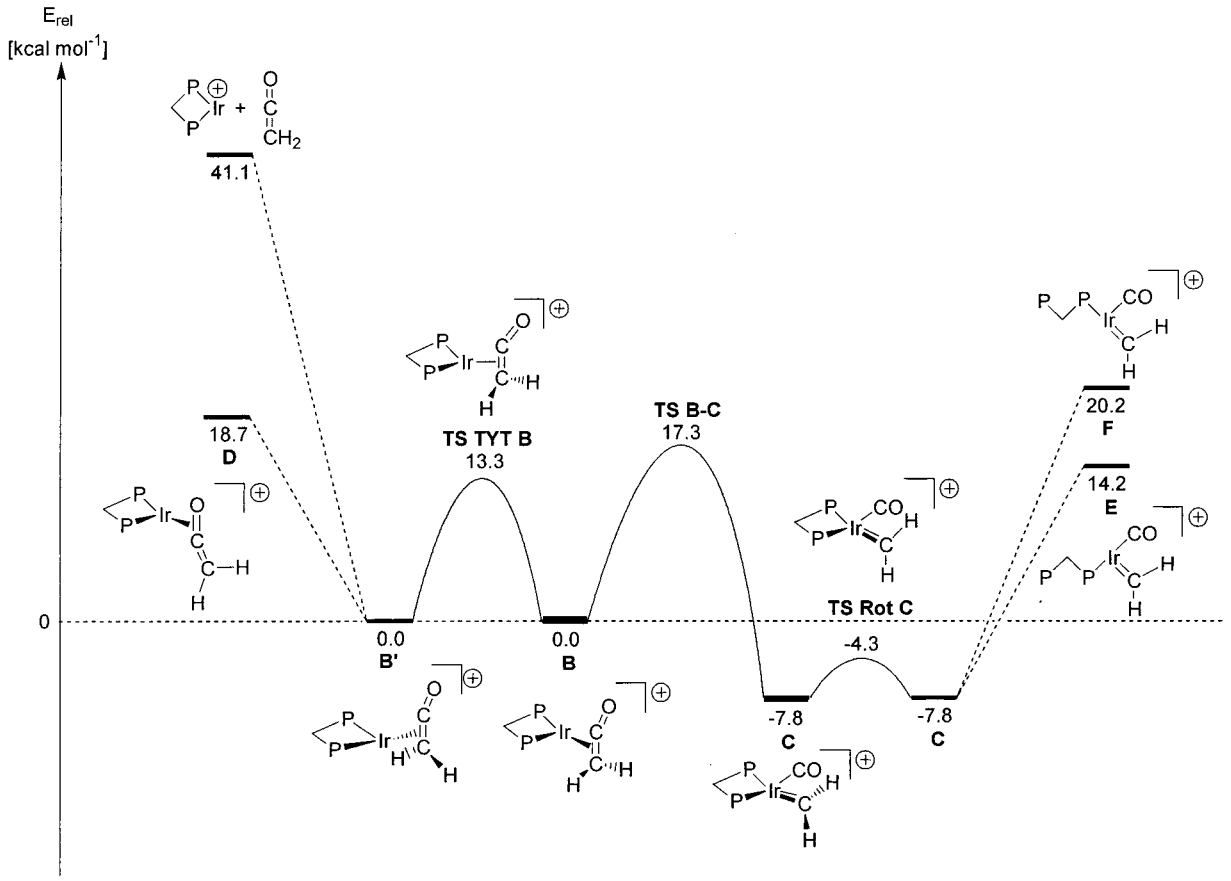

Figure 6. Calculated energy profile (B3PW91) for interconverting **B** and **C** and for related processes (see text).

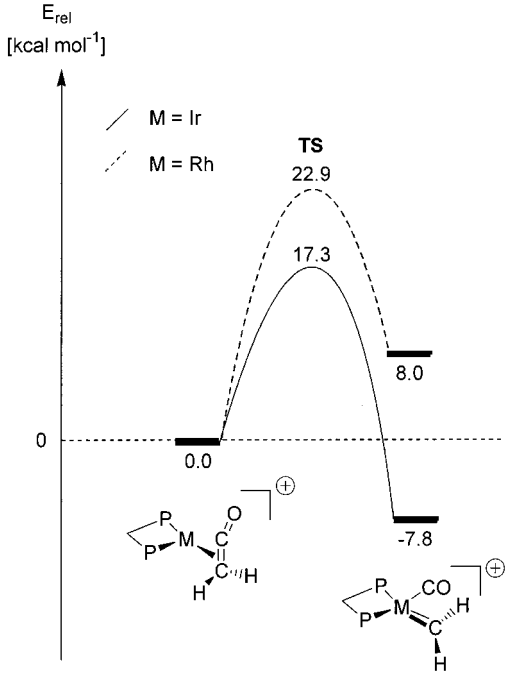

Figure 7. Computed energy profiles of ketene C═C cleavage/formation for Ir (**B**, **C**) and rhodium (**G**, **H**).

and C═C bond clevage have not been observed. We therefore calculated the C═C transformation processes also for the analogous rhodium model (κ^2-$H_2PCH_2PH_2$)-Rh[η^2-(*C*,*C*)-CH_2═C═O]$^+$ (**G**) and its carbene−carbonyl isomer (κ^2-$H_2PCH_2PH_2$)Rh(CH_2)(CO)$^+$ (**H**) (Scheme 3).

The computed (B3PW91) structures of **G** and **H** and the transition state **TS G-H** interconverting them are

Scheme 3

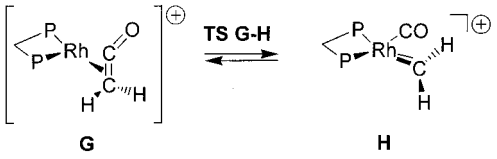

quite similar to the iridium complexes. Relevant geometric features are listed in Table 2.

Comparing the energy profiles of the C═C splitting/formation process on iridium and rhodium (Figure 7) reveals the inverted thermochemistry in the rhodium case.

In this case the ketene cation (κ^2-$H_2PCH_2PH_2$)Rh[η^2-(*C*,*C*)-CH_2═C═O]$^+$ (**G**) is favored by 8.0 kcal mol^{-1} compared to the carbene carbonyl complex (κ^2-H_2PCH_2-PH_2)Rh(CH_2)(CO)$^+$ (**H**), whereas the iridium ketene complex **B** is disfavored by 7.8 kcal mol^{-1}. This reflects the expected stronger Ir−C bonds compared to Rh. Furthermore, for Rh the activation barrier interconverting **G** and **H** via transition state **TS G-H** is higher than in the Ir case (22.9 kcal mol^{-1} compared to 17.3 kcal mol^{-1}) and lower for the reverse reaction (14.9 kcal mol^{-1} compared to 25.1 kcal mol^{-1}). The computed binding energy of the ketene ligand to the metal fragment in **G** amounts to 32.8 kcal mol^{-1} compared to 41.1 kcal mol^{-1} in the iridium system (24.7 kcal mol^{-1} with BSSE correction). The different bonding strengths of Rh versus Ir are also reflected in different bond lengths. The stronger back-bonding properties of Ir are obvious in the longer C═C bond of the ketene ligand in **B** compared to **G** (1.413 vs 1.392 Å). They are also

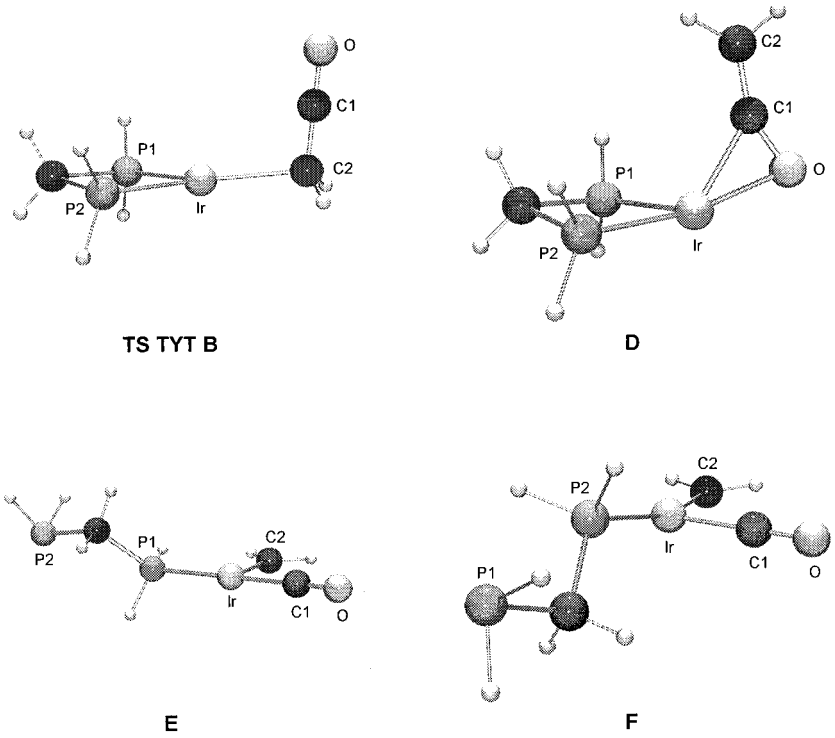

Figure 8. Calculated structures (B3PW91) of **TS TYT B**, **D**, **E**, and **F**.

Table 2. Relevant Bond Lengths [Å] and Angles [deg] of the Calculated Rhodium Structures G, TS G-H, and H (Atom Numbering Like in Figure 3)

parameter	G	TS G-H	H
Rh−P1	2.206	2.293	2.398
Rh−P2	2.367	2.429	2.488
Rh−C1	2.175	1.877	1.911
Rh−C2	2.106	1.916	1.875
C1−C2	1.392	1.893	2.674
C1−O	1.167	1.155	1.140
O−C1−C2	164.3	134.7	136.3
C1−Rh−C2	37.9	59.9	89.9
Rh−C1−O	127.4	160.1	178.9
P1−Rh−P2	73.8	71.7	69.0

apparent in the shorter Ir−CO distance in **C** (1.899 vs 1.911 Å in **H**) and the slightly elongated CO bond (1.144 vs 1.140 Å), in agreement with a reduced computed stretching frequency (ν_{CO} = 2176 cm^{-1} in **C** vs 2189 cm^{-1} in **H**; uncorrected).

Our calculations suggest that reversible ketene C=C bond cleavage should not be observable for rhodium systems with this type of ligand set.

Finally we want to address an interesting NMR coalescence phenomenon caused by some dynamic process which carbene complex **3** undergoes in solution. It was observed experimentally that some of the NMR line shapes of **3** varied with changes in sample temperature. To explore the exchange process that was occurring, **3**-^{13}CO was made with a high enrichment of ^{13}C in the CO ligand, starting with complexation of $Ph_2C{=}{}^{13}C{=}O$ to the (κ^2-dtbpm)IrCl fragment to give **1**-^{13}CO,[45] followed by treatment with $AgPF_6$. For this material, over a temperature range of −20 to +80 °C resonances for the protons in the C_6H_5 and PCH_2P groups remained sharp, whereas signals for the *t*-Bu protons changed in appearance. At low temperature in CD_2Cl_2, two large upfield doublets in the ^{1}H NMR spectrum at 1.47 ($^3J_{HP}$ = 14.7 Hz, 18 H) and 1.07 ppm ($^3J_{HP}$ = 14.9 Hz, 18 H) could be ascribed to the two different protons of (t-Bu)$_2$P units, one *trans* to carbene, the other *cis*. These signals broadened as the sample was warmed to near room temperature. At 80 °C only one single sharp doublet was observed for a sample in $ClCD_2CD_2Cl$. Significantly, when observed on a 200 MHz spectrometer, the coalescence temperature for these signals was the same in both chlorinated solvents, despite some difference in dielectric constant (10.37 for $ClCH_2CH_2Cl$ and 8.93 for CH_2Cl_2).[46] In the ^{31}P NMR spectrum (CD_2Cl_2, 80.95 MHz) of complex **3**-^{13}CO below 0 °C, the expected pattern of sharp peaks for the static structure was seen: in addition to the septet for free PF_6^-, there were two signals, one doublet of doublets (ascribed to the P *trans* to ^{13}CO) at −15.14 ($^2J_{PPcis}$ =17.6 Hz, $^2J_{CPtrans}$ = 91 Hz) and a second doublet of doublets (ascribed to the P *cis* to ^{13}CO) at −7.76 ppm ($^2J_{PPcis}$ =17.6 Hz, $^2J_{CPcis}$ = 11.9 Hz). Warming the sample above 0 °C led to broadening and coalescence, although even at 80 °C, the one resonance seen was still broad. Line shape analysis of the proton and phosphorus NMR spectra, followed by least-squares analysis of plots of ln k versus T^{-1}, led to values for activation energies E_a of 15.3 ± 0.3 and 14.5 ± 1.2 kcal mol^{-1}, respectively, with preexponential factors A = 9.8 ± 5.0 × 10^{12} and 3 ± 6 × 10^{12} s^{-1}, respectively (Table 3). Each pair of values is identical within experimental uncertainty, although the proton NMR data are taken as more reliable.

To explain the coalescence of the resonances due to the P(t-Bu)$_2$ groups of **3** observed in ^{1}H and ^{31}P{^{1}H} NMR spectra, one can consider two possible pathways of exchanging the P nuclei, which we treated theoretically. One possibility would be a ring-opening process

(45) Grotjahn, D. B.; Collins, L. S. B.; Wolpert,M.; Bikzhanova, G. A.; Lo, H. C.; Combs, D.; Hubbard, J. L. Manuscript in preparation.

(46) Reichardt, C. *Solvents and Solvent Effects in Organic Chemistry*, 2nd ed.; VCH: Weinheim, 1988; p 409.

Table 3. Rates of Interconversion at Various Temperatures[a]

temp, °C	^{31}P	^{1}H
−20	10.5 (1.0)	
−15		0.00 (0)
5	19 (1)	
10		19.7 (1.0)
15	32 (5)	
20	50 (5)	42 (1)
30		96 (1)
33		113 (1)
36		144 (3)
40	100 (5)	210 (10)
50	510 (10)	330 (10)
60	940 (30)	960 (20)
70	1750 (100)	2000 (100)
80	5550 (500)	3500 (200)

[a] Rates determined by visual comparison of NMR line shapes obtained for the indicated nuclei experimentally and calculated using WINDNMR. Estimated uncertainties of rates are listed in parentheses. No rate means no spectrum was acquired at that temperature.

Scheme 4

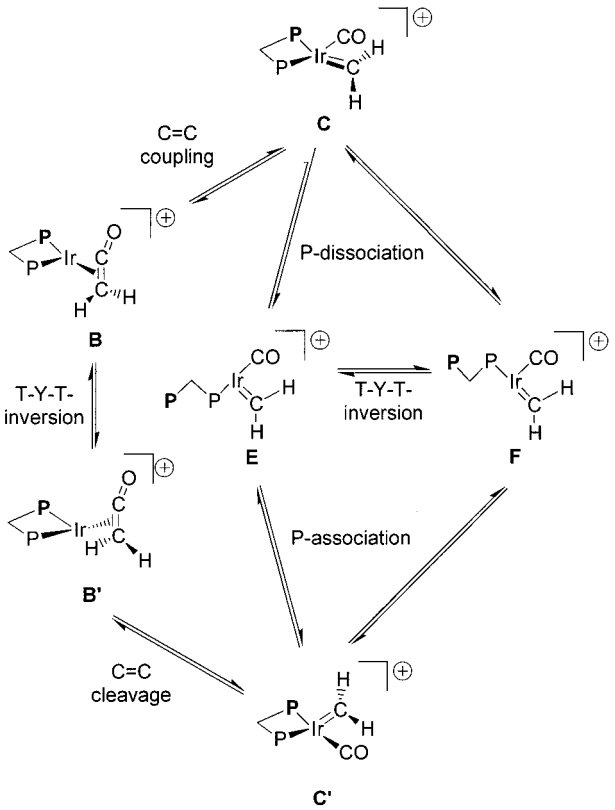

of the chelate ring in **C** leading to **E** or **F** (Scheme 4, Figure 8). These two species are calculated to be 22.0 and 28.0 kcal mol^{-1} higher in energy than **C**, respectively (Figure 6). Conversion of T-shaped **E** to T-shaped **F** and vice versa via an energetically even less favorable Y-shaped transition state with subsequent ring closure to generate **C′** would then exchange the two P atoms. Thus, the activation barrier has to be at least as high as the highest one of these two values.

An alternative pathway is the T-shaped to T-shaped interconversion of enantiomers **B** and **B′**, again through a Y-shaped (C_s) transition state (**TS TYT B**) with an activation barrier of 13.3 kcal mol^{-1}. For this pathway the C═C coupling reaction generating **B** or **B′** from **C** (25.1 kcal mol^{-1}) necessarily has to precede the inversion and will be the rate-determining step. From an overall energy point of view this process seems to be most plausible for the P(*t*-Bu) exchange observed by NMR for complex **3**.

Conclusions

DFT and ONIOM calculations for the first transition metal η^2-(*C,C*) ketene complex which allows observation of C−C double bond splitting and formation at a single metal center correctly reproduce the structural features of all compounds studied by experiment. A qualitative symmetry analysis based upon EH-MO correlation diagrams shows the electron-rich late transition metal center Ir(I) with d^8 electron configuration and two *cis*-ligands to provide the appropriate template for a symmetry-allowed C═C ketene double bond splitting process.

The DFT and QM/MM computed energetics for model compounds and for the real systems fully support an interpretation of experimental data in which chloride abstraction from the ketene complex (κ^2-dtbpm)IrCl[η^2-(*C,C*)-Ph_2C═C═O] (**1**) creates a three-coordinate, cationic, nonobservable 14-electron intermediate (κ^2-dtbpm)Ir[η^2-(*C,C*)-Ph_2C═C═O]$^+$ (**2**), which rearranges to (κ^2-dtbpm)Ir(CPh_2)(CO)$^+$ (**3**). The computed energies for the unsubstituted dhpm model systems reflect that the ketene C−C double bond of the proposed intermediate (κ^2-dtbpm)Ir[η^2-(*C,C*)-Ph_2C═C═O]$^+$ (**2**) can indeed readily be cleaved (computed barrier of only 17.3 kcal mol^{-1} for model **B**) leading to the thermodynamically favored carbene carbonyl isomer (κ^2-dtbpm)Ir(CPh_2)(CO)$^+$ (**3**). Strong metal to ligand back-bonding makes C═C splitting energetically feasible and explains the thermodynamic preference for the carbene−carbonyl Ir complex. The reverse coupling reaction has a barrier of 25.1 kcal mol^{-1} for the simplified dhpm model (from **C** to **B**). This is in line with a re-formation of **1** upon addition of chloride anions, by trapping the unfavored intermediate **2** out of the equilibrium and shifting the system back toward the neutral ketene chloride complex **1**. When Rh replaces Ir as the metal center, a high barrier toward ketene cleavage and reversed thermodynamic stability of the two isomers is predicted from DFT. The computed energies of the Ir system also explain the observed coalescence of the P(*t*-Bu) signals in the NMR spectra of the carbene carbonyl system **3** upon raising the temperature to 80 °C, because **C** (and thus **3**) can undergo C−C coupling in a rate-determining step (25.1 kcal mol^{-1}) to **B** or **B′**, followed by relatively facile T−Y−T inversion with a low barrier of 13.3 kcal mol^{-1}. This sequence exchanges the two P nuclei, leading to coalescence of the ^{31}P and *t*-Bu signals in complex **3**. An alternative mechanism of P exchange by cleaving one of the Ir−P bonds is calculated to require much more energy and therefore is much less probable.

Acknowledgment. This work was generously supported by the Deutsche Forschungsgemeinschaft (SFB 247 and Graduate College Fellowship for H.U.) and by the Fonds der Chemischen Industrie. Acknowledgment is made by G.A.B. and D.B.G. to the donors of the Petroleum Research Fund, administered by the ACS, for partial support of this research, and by H.U. and P.H. to the PROCOPE-program of the European Union.

We also wish to thank Prof. O. Eisenstein and Dr. E. Clot (Montpellier) for valuable discussions. Earlier, related theoretical work (EHT) on olefin and ketene bond-breaking and bond-forming at metal fragments, which formed a valuable and informative background for this study, has been performed by H. R. Schmidt.[23]

Supporting Information Available: Computational details of the extended Hückel calculations. Tables of relevant interatomic distances and angles for the computed species **A**, **B**, **TS B-C**, **C**, and **TS Rot C** obtained with B3LYP and BP86. Cartesian coordinates for calculated (B3PW91) structures **A**−**H**, the transition state structures, and the structures from ONIOM calculations of **1**−**3**. This material is available free of charge via the Internet at http://pubs.acs.org.

OM010503T